Journal of Food Measurement and Characterization (2021) 15:4849–4857
https://doi.org/10.1007/s11694-021-01054-x

ORIGINAL PAPER

# Cysteamine-mediated upconversion sensor for lead ion detection in food

Yi Xu[1] · Felix Y. H. Kutsanedzie[2] · Shujat Ali[3] · Pingyue Wang[1] · Chunyan Li[1] · Qin Ouyang[1] · Huanhuan Li[1] · Quansheng Chen[1]

Received: 19 April 2021 / Accepted: 28 June 2021 / Published online: 10 July 2021


## Abstract

Lead ion ($Pb^{2+}$) accumulation in food consumed by humans and animals possess health threats and effects. The development of a senor for its monitoring at its minutest accumulation in edible materials becomes an antidote to safeguarding human lives. A fabricated fluorescence-based sensor made of carboxyl modified upconversion nanoparticles (UCNPs), gold nanorods (GNRs), and cysteamine (Cys) were used as energy donor, receptor and a bridge respectively for the rapid sensing of $Pb^{2+}$ in Matcha. The UCNPs-Cys-GNRs sensor showed weak fluorescence signals due to the FRET, and was inhibited in the presence of $Pb^{2+}$ to form a complex with Cys, and the consequent recovery of fluorescence signals. Under optimized conditions, a good linear relationship was established between the relative fluorescence intensity and $Pb^{2+}$ concentrations from 1 to 100 μM with a low detection limit (LOD) of 0.5 μM. The developed sensor was applied to detect $Pb^{2+}$ in Matcha samples with recoveries within 93.99—102.16% and relative standard deviations (RSD) < 8%. Satisfactory results ($p > 0.05$) were obtained upon validation using a standard inductively coupled plasma mass spectrometry (ICP-MS).

**Keywords** Matcha · Food analysis · Upconversion nanoparticles · Fluorescence · Lead ion

## Highlights

- UCNPs-cysteamine-gold nanorods FRET sensor for fabricated for Pb2+ detection
- The FRET sensor developed was deployed to detect Pb2+ in food samples at μM level
- A low LOD of 0.5 μM was achieved by the FRET sensor when deployed

✉ Huanhuan Li
jiona1044@ujs.edu.cn

✉ Quansheng Chen
qschen@ujs.edu.cn

[1] School of Food and Biological Engineering, Jiangsu University, Zhenjiang 212013, People's Republic of China

[2] Research and Innovation Centre/Mechanical Engineering Department, Accra Technical University, Accra, Ghana

[3] College of Electrical and Electronic Engineering, Wenzhou University, Wenzhou 325035, People's Republic of China

## Introduction

Health care-based products and health concerns are of utmost importance to consumers as a result of the consequent the economic and debilitating effects health threats they have on human [1–4]. Matcha is a known health care product patronized by consumers due to its characteristic bioactive ingredients and usage as "green tea" over years [5]. As a result of industrialization and urbanization, anthropogenic activities have seriously interfered ecosystem with resultant massive pollution of the atmosphere, waterbodies and soil with toxic materials such heavy metals and hazardous chemicals [6–8]. These heavy metals and hazardous chemicals are imbibed by plants roots and consequently accumulated in their body tissues as primary source of food and health product for humans as well as animals within the food chain and web. The resultant food harvested from plants grown in such soils or environment are unavoidable consumed by humans and thus exposing them to myriads of diseases with debilitating effects. Matcha as a plant used for tea, is known to continuously absorb heavy metals from its surrounding environment and soil during it growth process via roots absorption and leaves infiltration. These heavy

metals become accumulated in the fresh leaves plucked and used as tea leaves at maturity above required limits or thresholds [9]. Heavy metals levels quantification in food materials is a vital safety indicator or index. Lead ion ($Pb^{2+}$) has been reported to be one of the most toxic which accumulates in Matcha and its products. Match and Matcha products contaminated by $Pb^{2+}$ pose health threats to the human nervous, blood and cardiovascular systems when ingested into the human body [10]. Sequel, 0.5 mg/kg has been established as the maximum residue limits (MRLs) of $Pb^{2+}$ in Matcha based on the National Standard of PR China [11], with variations in other countries and jurisdictions.

Currently, conventional methods such as inductively coupled plasma emission spectrometry (ICP-AES), inductively coupled plasma-mass spectrometry (ICP-MS) and atomic absorption spectrometry (AAS) are widely being used for the detection of heavy metal detection in various materials [12, 13]. However, the high operational cost, the intensive skilled labour required, and the complexity of the pretreatment procedures associated with these methods prevent their use for real-time detection. These aforementioned constraints have been gradually addressed by the introduction of new sensing systems like colorimetric sensors, fluorescent sensors, electrochemical sensors and surface-enhanced Raman scattering (SERS) sensors [14–17]. For instance, fluorescent based sensors have been reported to possess high sensitivity and analytical precision in detecting heavy metal ion in food materials [18–20]. Fluorescent sensors are fabricated with organic fluorescence dye, quantum dots and carbon dots, etc. However, fluorescent sensors are generally grouped into twofold—downconversion and upconversion fluorescent sensors. The former fluorescence sensors are usually fabricated using organic molecules, quantum dots (QDs) and carbon dots (CDs), which reportedly suffers from high background fluorescence of endogenous chromophores in samples; however, the latter group of fluorescence sensors are fabricated with rare earth-doped upconversion nanoparticles (UCNPs), established to possess outstanding features such as high Stokes shift, resistance to photobleaching and quantum yields. Furthermore, UCNPs have high chemical stability, low cytotoxicity and stable luminescence properties capable of converting long-wavelength to short-wavelength light to prevent background autofluorescence and improved sensitivity [21]. These unique properties of UCNPs have enabled their successful application for the fabrication of sensors for the detection of heavy metal ions in various materials [22–24].

Several works have been carried out and reported as regard fluorescent sensors fabrication. For example, a turn-on nano-fluorescence sensor for mercury ($Hg^{2+}$) detection based on FRET between aptamer modified UCNPs and gold nanoparticles (GNPs) was developed by Liu et al. with a linear range of 0.2—20 µM limit of detection (LOD) of 60 nM obtained [18]. Additionally, Vijayan et al. proposed a UCNPs based signal-amplication sensor for $Hg^{2+}$ detection. In view of that, DNA-conjugated UCNPs was used as $Hg^{2+}$ capture unit via the interaction between the thymine bases from DNA and $Hg^{2+}$ to form a thymine—$Hg^{2+}$- thymine complex, which achieved a LOD of 0.14 nM [24]. Wang et al. reported a RFET based biosensor using UCNPs as donors and Au NPs as receptors to form an assembly via complementary aptamer hybridization for $Pb^{2+}$ detection [25]. The FRET breaks in the presence of $Pb^{2+}$ to affect the dissociation of donors and receptors. The afore-stated fabricated sensor yielded a LOD of 4.1 nM when tested in buffer solution. Conversely, complexity of aptamer modification operations, render the practical application of UCNPs-based sensors difficult due the unstable nature of aptamers in real-life situations. Its therefore germane to probe into the fabrication of a simpler and more efficient UCNPs-based sensors for $Pb^{2+}$ detection.

This paper focused on the design and application of a label-free UCNPs- cysteamine-gold nanorods FRET sensor for the detection of $Pb^{2+}$ in food samples. As shown in Scheme 1, a novel carboxyl modified UCNPs (UCNPs-COOH) was designed and fabricated as energy donor, gold nanorods (GNRs) synthesized as energy acceptor, and cysteamin (Cys) used as a bridge to connect the donor and

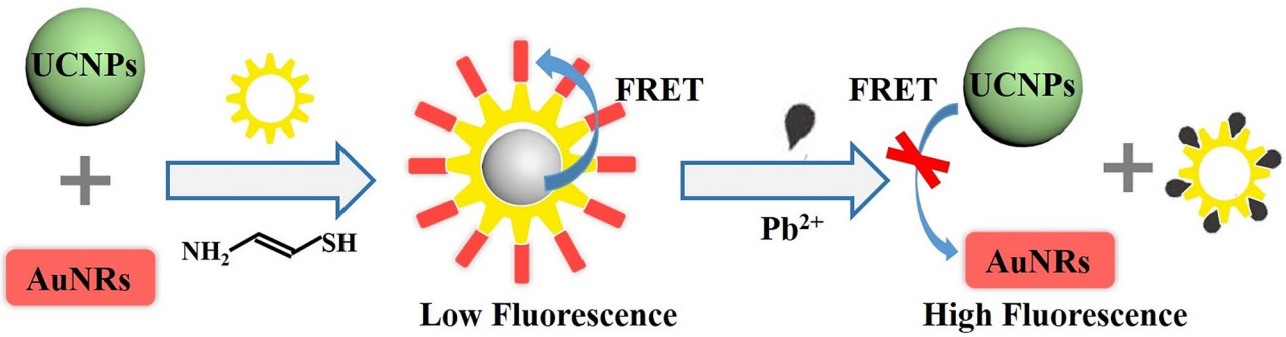


**Scheme 1** Schematic description of the UCNPs-Cys-AuNRs fluorescence nanosensor for $Pb^{2+}$ detection

acceptor through an amide and gold sulfhydryl bond respectively. The resultant complex displayed a weak fluorescence signal due to the FRET. However, the signal amplified in the presence of $Pb^{2+}$ due to its complexation with Cys. This resulted in the release of the latter (Cys) from the assembly, and the subsequent interruption of the RFET to emit strong fluorescence signal. Thus, the intensity of the fluorescence signal is expected to be stronger with increasing concentration of the $Pb^{2+}$ to enable the design of a Cys modulated UCNPs biosensor for the detection of $Pb^{2+}$. As far as we know, this work reports the first attempt of using the developed UCNPs- cysteamine-gold nanorods FRET sensor for the detection of $Pb^{2+}$ in Matcha, with great promise also shown for its possible deployment for the determination of other heavy metal ions with better stability and reproducibility. The developed sensor is expected to be possibly deployed for the detection of $Pb^{2+}$ in real samples, as well as provide an innovative idea for the design of other label-free sensors for heavy metal ion detection.

## Experimental

### Materials

Analytical grade solvents and materials were used in this work, without further purification. Materials such as Yttrium chloride hexahydrate ($YCl_3\%6H_2O$, 99.99%), erbium (III) chloride hexahydrate ($ErCl_3\%6H_2O$, 99.99%), and ytterbium (III) chloride hexahydrate ($YbCl_3\%6H_2O$, 99.99%) were all obtained from Aladdin Industrial Inc. (Shanghai, China). Oleic acid (OA, 90%), 1-Octadecene (ODE, 90%), ammonium fluoride ($NH_4F$, 96%), trisodium citrate dihydrate (99%), and chloroauric acid hydrated ($HAuCl_4{\cdot}4H_2O$) were procured from Macklin Biochemical Technology Co., Ltd (Shanghai, China). Methanol, sodium hydroxide, ethanol, cyclohexane, diethylene glycol, toluene, cetyltrimethylammonium bromide (CTAB, 99%), sodium borohydride, sodium oleate, silver nitrate, hydrochloric acid, ascorbic acid, cysteamine and lead nitrate were all acquired from Sinopharm Chemical Reagent Co., Ltd. (Shanghai, China). Deionized water obtained via a smart-s ultrapure water system was utilized throughout the conduct of the experiment**.**

### Instruments and characterizations

The confirmation of the size and morphology of UCNPs and GNRs were done utilizing a JEOL JEM-2100 (HR) high-resolution transmission electron microscope (HR-TEM; JEOL Ltd., Japan) at 200 kV accelerating voltage. The crystalline phases of the synthesized nanomaterials were characterized by X-ray powder diffractometer (XRD) patterns based on a D8 Advance (Germany) X-ray diffractometer at a 5°/min scanning rate in the 2θ range from 10° to 60°. UV–Vis absorption spectrum was recorded with Agilent 8453 Ultraviolet–visible (UV–Vis) spectrophotometer (Agilent Technologies Inc.). The Fourier transform infrared (FT-IR) spectra were all obtained using a Nicolet Nexus 470 Fourier transform infrared spectrophotometer (Thermo Electron Co., U.S.A.) based on the potassium bromide method.

### Synthesis and modification of UCNPs

Oil soluble UCNPs were initially synthesized via a high temperature thermal decomposition technique with some modifications [26]. An amount of 0.78 mmol $YCl_3{\cdot}6H_2O$, 0.2 mmol $YbCl_3{\cdot}6H_2O$, and 0.2 mmol $ErCl_3{\cdot}6H_2O$ were dissolved in 5.0 mL methanol and then transferred into a three (3) round bottomed flask containing 6.0 mL oleic acid and 15.0 mL 1-Octadecene. The mixture was heated to the 160 ℃ and maintained for 30 min with stirring under argon protection of argon. After it was cooled to 50 ℃, 4.0 mmol $NH_4F$ and 2.5 mmol NaOH solution in methanol was dropped in the resultant mixture under stirring. Subsequently, it was heated to 70 ℃ under stirring for 40 min until the methanol evaporated. The temperature of the content was raised to 100 ℃ and sustained for 10 min, and further raised to 300 ℃ for 1.5 h to form nanocrystals. Upon the completion of the reaction, the content was cooled to room temperature, and the resultant product washed with cyclohexane-ethanol solution (2:1) and centrifuged at 8000 rpm. The OA-UCNPs were obtained after drying in a vacuum oven at 70 ℃ for 12 h.

In fabricating a detection system for $Pb^{2+}$, the OA-UCNPs synthesized was made water-soluble. This was realized by modifying the surface of OA-UCNPs with carboxyl groups via ligand exchange process with oleic acid citrate [27]. During the process, 2 mmol sodium citrate was dissolved in 15 mL diethylene glycol and heated subsequently for 30 min under argon condition to 110 ℃. After cooling the resultant content to 60 ℃, 10 mg OA-UCNPs deposited in cyclohexane – toluene solution (v/v = 3:2) was thereafter added and heated to 130 ℃ in order to evaporate the cyclohexane and toluene. Afterward, the temperature was further raised to 180 ℃ under argon condition until yellow colour was observed for the resultant solution. The product obtained (UCNPs-COOH) was subsequently washed thrice with 50% ethanol solution and centrifuged for 15 min at 12,000 rpm. The UCNPs-COOH was finally dispersed in ultrapure water and stored at 4 ℃.

### Synthesis of AuNRs

A modified seed mediated growth technique was utilized for the synthesis of Gold nanorods (AuNRs) [28]. This was done by mixing 2 mL $HAuCl_4$ (0.5 mM) with 2 mL CTAB

solution (0.2 M). A volume of 0.4 mL $NaBH_4$ solution (0.06 M) was added and stirred vigorously for 2 min until a color change from yellow to pale brown was observed. The resultant seed solution obtained was stored at 25 ℃ for usage. A mixture solution of 0.56 g CTAB, 0.10 g sodium oleate and 20 mL ultra-pure water was kept at 50 ℃ for 30 min, and then cooled to 30 ℃. Subsequently, 1.92 mL $AgNO_3$ (4 mM) was added to react with it for 15 min; and thereafter 20 mL $HAuCl_4$ (1 mM) added to further react for another 90 min. When a change in the color of the solution from dark yellow to colorless was observed, 0.17 mL HCl solution (12.1 M) was added to adjust the pH value, and the resulting content stirred steadily for 15 min. Subsequently, 0.10 mL solution of fresh ascorbic acid (0.06 M) was added while stirring briskly for 30 s. Lastly, 64 µL seed growth solution was added under stirring for 30 s and heated at 30 ℃ overnight to finally obtain the AuNRs.

### Fabrication of UCNPs-Cys-AuGRs label-free based fluorescence sensor

The core principles underpinning the fabrication of UCNPs-Cys-AuGRs label-free based fluorescence sensor includes: the ability of amino and sulfhydryl groups of cysteamine to form amide bond and Au–S bond to create UCNPs; as well as Cys and AuNRs to combine; the fluorescence quenching effect of AuNRs on UCNPs; the complex effect between $Pb^{2+}$ and Cys, the capability of the formed complex to interfere with the fluorescence quenching process and induce the fluorescence signal of UCNPs to be reactivated. The detailed design of the core principle underpinning the fabricated sensor is shown in Scheme 1. In the absence of the target $Pb^{2+}$, Cys functions as a bridge to form both amide bond with carboxyl from UCNPs, and Au–S bond through its sulfhydryl group with AuNRs. The complex formed exhibits weak fluorescence signals due to the FRET. However, in the presence of $Pb^{2+}$, the complexation between Cys and $Pb^{2+}$ produces interference in the FRET process and also induces the recovery of fluorescence signal of the sensor. With the increase in the $Pb^{2+}$ concentration, the fluorescence intensity of the system surges steadily. Thus, indirect relationship between the $Pb^{2+}$ concentration and the fluorescence signal intensity of the system established, enabling a quantitative analysis of the target substance to be realized. In order to accomplish that, the synthesized AuNRs were diluted thirty (30) times with Britton Robinson (BR) buffer solution, and 300 µL of diluent mixed with a certain concentration of Cys at 25 ℃. Subsequently, 300 µL of UCNPs-COOH was added to the afore-stated to make UCNPs-Cys-AuGRs detection system. Thereafter, various concentrations of $Pb^{2+}$ (100 µL) were introduced and incubated at 25 ℃. The fluorescence spectra of the reaction solution with different concentrations of $Pb^{2+}$ were finally collected based on 980 nm excitation using the preheated upconversion fluorescence spectrometer.

### Determination of $Pb^{2+}$ in real matcha samples

Matcha samples bought from local Auchan supermarket were pretreated as follows. A mass of 0.5 g Matcha samples were weighed and placed in microwave digestion tank with 10 mL of nitric acid. The microwave digestion tank was moved into the microwave digestion oven and heated to 120 ℃ for 5 min, raised to 160 ℃ for further 10 min, and then to 180 ℃ for 20 min to enable the digestion of the samples. When cooled, the digestion tank was moved out and kept in a constant temperature oil bath within the range of 140—160 ℃ to enable the acid to evaporate and reduce to 1 mL. The content of the digestion tank was thereafter membrane-filtered. Consequently, the sodium hydroxide prepared was added to the filtrate drop by drop to adjust the pH value to 7.4 and the digestion solution diluted with PBS buffer (2 mL), and the different standard $Pb^{2+}$ concentrations of samples added and mixed for usage. Lastly, the fluorescence spectral data of the spiked samples were obtained, and their respective $Pb^{2+}$ contents in the above spiked samples predicted using the established linear relationship based on the recovery rates computed. Additionally, Matcha tea samples adulterated with $Pb^{2+}$ were determined by the designed sensor and compared with results from traditional atomic absorption spectrometry following the same pretreatment process. The detection of the $Pb^{2+}$ content of the pretreated spiked samples using the inductively coupled plasma mass spectrometry (ICP-MS). In the process, 0.5 g Matcha samples were put into the microwave digestion inner pot followed by the addition of 1 mL standard $Pb^{2+}$ solution of the concentrations (0, 50, 100, 500, and 1000 µg/L) respectively and 9 mL of nitric acid. The content was covered for an hour and then digested. The digestion solution was heated at 100 ℃ for 30 min and its constant volume set to 50 mL for usage. Finally, the blank solution and the sample solution were injected into the inductively coupled plasma mass spectrometry (ICP-MS), and the signal response values of the elements and the internal standard elements were measured.

## Results and discussion

### Characterization of UCNPs-COOH

Upconversion nanoparticles (UCNPs) were synthesized by high temperature thermal decomposition method. The surface of the oleic acid coated UCNPs was replaced by citrate via the ligand exchange method, giving the nanoparticles good dispersion in water. Figure 1A shows a typical TEM image of OA-UCNPs with a diameter of about 20 nm. The

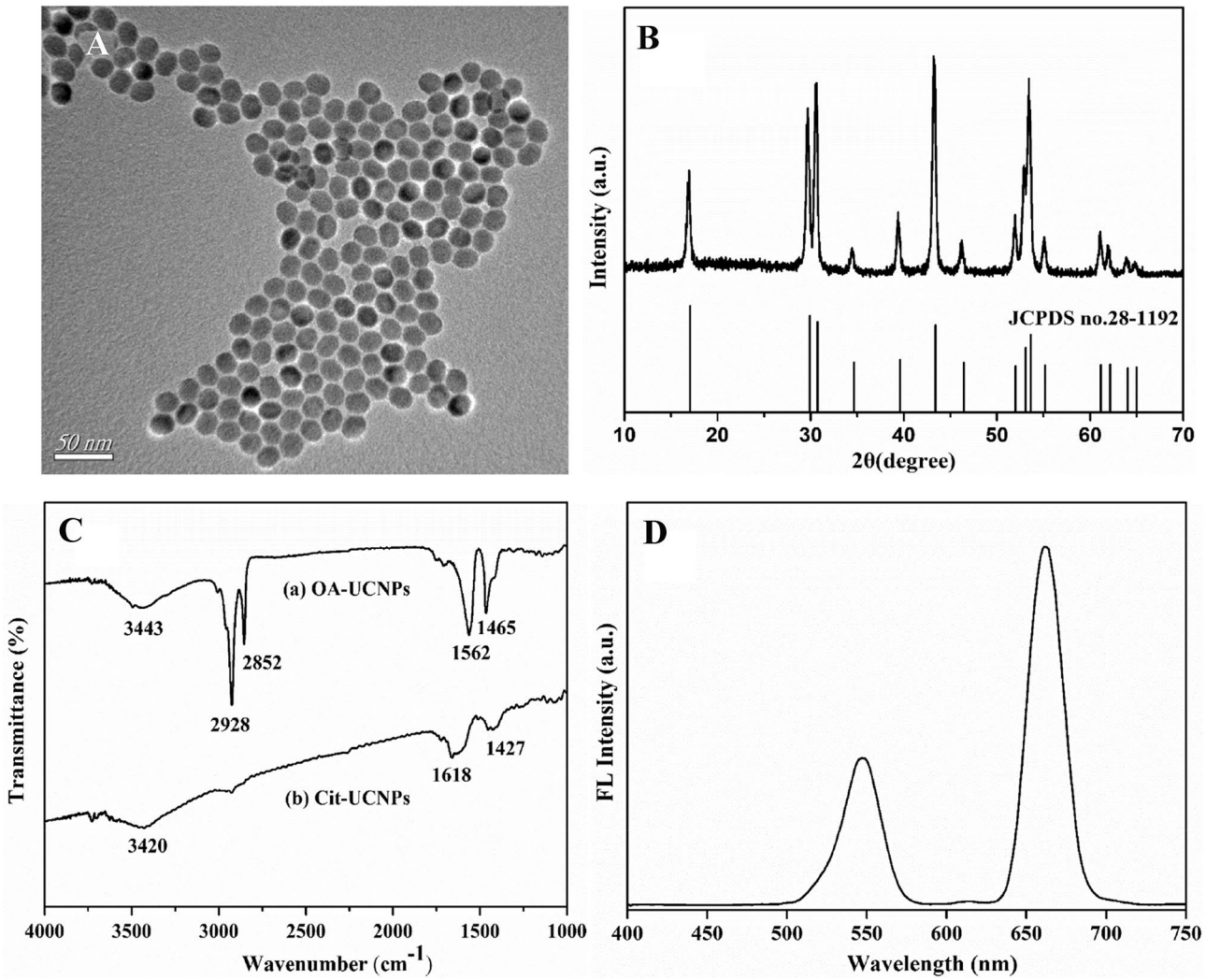


**Fig. 1** TEM image (**A**), XRD pattern (**B**), FT-IR spectroscopy (**C**) and fluorescent emission spectra (**D**) of UCNPs

hexagonal phase of OA-UCNPs was further confirmed by X-ray diffraction as captured in Fig. 1B. As a fluorescent marker, UCNPs gave excellent luminescent properties and also good hydrophilic properties for practical application. The surface functionalization of UCNPs was realized by grafting carboxyl group using the ligand exchange method. FT-IR analysis was conducted to verify the surface groups of the modified UCNPs. Figure 1C captures the characteristic peaks of OA-UCNPs. Five obvious peaks at 2928 $cm^{-1}$, 2852 $cm^{-1}$, 1562 $cm^{-1}$, 1465 $cm^{-1}$ and 3443 $cm^{-1}$ were noticed and ascribed to asymmetrical and symmetrical stretching vibration of methylene (- $CH_2$ -) in hydrophobic long alkyl chain of oleic acid; symmetrical and asymmetrical stretching vibration of carboxyl group in oleic acid ligand; and vibration of hydroxyl group (- OH) contained in oleic acid ligand. After ligand exchange, the peaks related to oleic acid at 3443, 2928 and 2852 $cm^{-1}$ vanished, while an observable peak at 3420 $cm^{-1}$ related to the stretching vibration of hydroxyl groups in water and citric acid, and the band related to carboxyl group shifted to 1618 and 1427 $cm^{-1}$ respectively [27]. These results reveal that the UCNPs surface was successfully coated with the citrate. Figure 1D shows the fluorescence spectra of the water-soluble UCNPs under 980 nm laser excitation. Two characteristic emission peaks at 547 nm and 660 nm corresponding to the energy level transition of $Er^{3+}$ ions from the excited state ($^4S_{3/2}$ and $^4F_{9/2}$) to the ground state ($^4I_{15/2}$) were seen.

## Characterization of AuNRs

Gold nanorods (AuNRs) were synthesized by seed mediated growth method and characterized by UV–Vis absorption spectroscopy and TEM. As shown in Fig. S1A, AuNRs have a characteristic UV absorption peak at 527 nm, which overlaps with the UCNPs emitted fluorescence peak of at 547 nm, satisfying the condition for fluorescence resonance

energy transfer. The characteristic fluorescence peak at 547 nm was hence selected as the reporter signal in the experiment for subsequent data analysis. Transmission electronic microscope (TEM) was used to characterize the size and morphology of AuNRs as shown in Fig. S1B. The AuNRs synthesized appeared rod-shaped with uniform morphology and good dispersion. The sizes of the long and short axes of the nanorods were estimated to be 100 nm and 28 nm respectively.

## Optimization of detection conditions

Optimization of the detection conditions was carried out in order to obtain the best detection performance of the fabricated sensor. To do established that, the detection conditions such as the concentration of AuNRs, Cys and the $Pb^{2+}$ response time of the mixed system were optimized. The effect of the concentration of AuNRs was initially studied. Equal amount of Cys and UCNPs-COOH solution mixed with varied concentrations of 300 µL AuNRs independently (0, 2.5, 5, 10, 15, 20, 40, 60 pM) and the subsequent addition of 100 µL of water. The fluorescence signals of the various mixtures were recorded. As seen in Fig. 2A, the intensity of the UCNPs fluorescence signal steadily decreased with the increase in AuNRs concentration. When the AuNRs concentration exceeded 40 pM, the signal intensity became fairly stable. As a result, 40 pM AuNRs solution was selected as the best concentration for this experiment. The effect of Cys concentration on the developed UCNPs-based sensor was thereafter carried out. Varied concentrations of Cys solution (0, 50, 100, 200, 300, 400, 500, 600 µM), 300 µL UCNPs solution and 100 µL deionized water were added to 300 µL AuNRs. After simple mixing of the contents at 25 ℃, the fluorescence intensities of the mixed solutions were recorded. As captured in Fig. 2B, increase of Cys concentration triggered a steady decrease in the fluorescence intensity of UCNPs at 547 nm as a result of the increasing amount of UCNPs-Cys-AuNRs complexes. When the concentration was exceeded 500 µM, stability in the fluorescence intensity was observed. Based on that, 500 µM was selected as the best concentration of Cys for $Pb^{2+}$ detection. Furthermore, the response time of the sensor to detect $Pb^{2+}$ was optimized based on the stability in the fluorescence intensity of the mixed solution with time as the evaluation criterion. Under the optimal detection conditions, $Pb^{2+}$ were introduced into the mixed detection system. After incubation at 25 ℃ for 1, 2, 4, 6, 8, 10 and 12 min, the fluorescence spectral data of the mixed solution under different reaction times were collected. The variation curve for fluorescence intensity with time at 547 nm is shown in Fig. 2C. It can be observed that the detection system reacts rapidly with $Pb^{2+}$ at 25 ℃ while and the fluorescence intensity of the system remained unchanged. Thus, 1 min was selected as the best incubation time.

## Establishment of detection standard curve

Under the optimized experimental conditions, the upconversion fluorescence spectra of the mixed detection system were collected after adding series of $Pb^{2+}$ standard solutions of varied concentrations. Figure 3A shows the changes of UCNPs fluorescence spectra of the system after adding varied concentrations of $Pb^{2+}$. It is seen the Fig. 3A that increased amount of the target molecular concentration allows the gradual dissociation of Cys from the assembly, and the consequent steady enhancement of the fluorescence intensity of the mixture at 547 nm. Figure 3B shows the relationship between the relative fluorescence intensity $(F–F_0) / F_0$ (F and $F_0$ representing the fluorescence intensity value at 547 nm prior and post addition of $Pb^{2+}$) and $Pb^{2+}$ concentration. A linear regression equation was obtained for the relationship as $(F–F_0) / F_0 = 0.048\ x + 1.308$, $R^2 = 0.987$, and

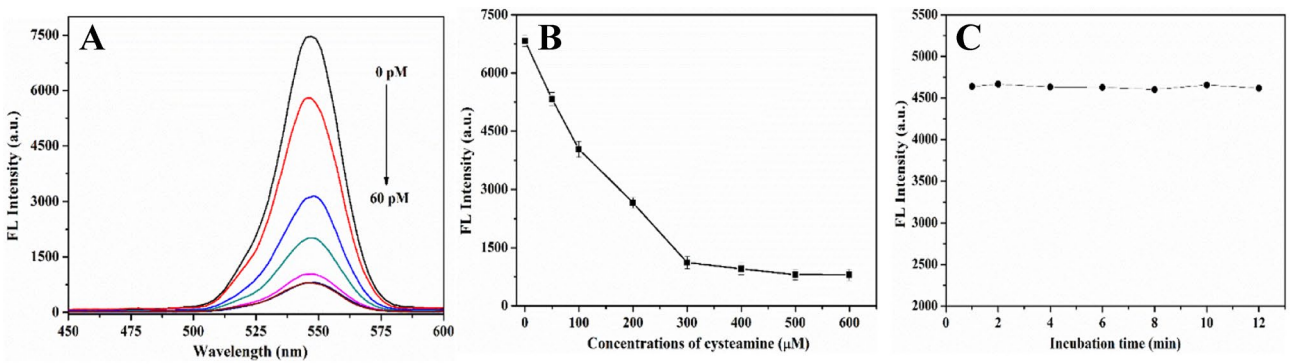


**Fig. 2** Fluorescence spectra of upconversion with addition of different concentrations of AuNRs (**A**), Fluorescence intensity of the system at different concentrations of cysteamine at 547 nm. Error bar = SD (n = 3) (**B**) and Optimization of incubation time after adding Pb2 + to the detection system (**C**)

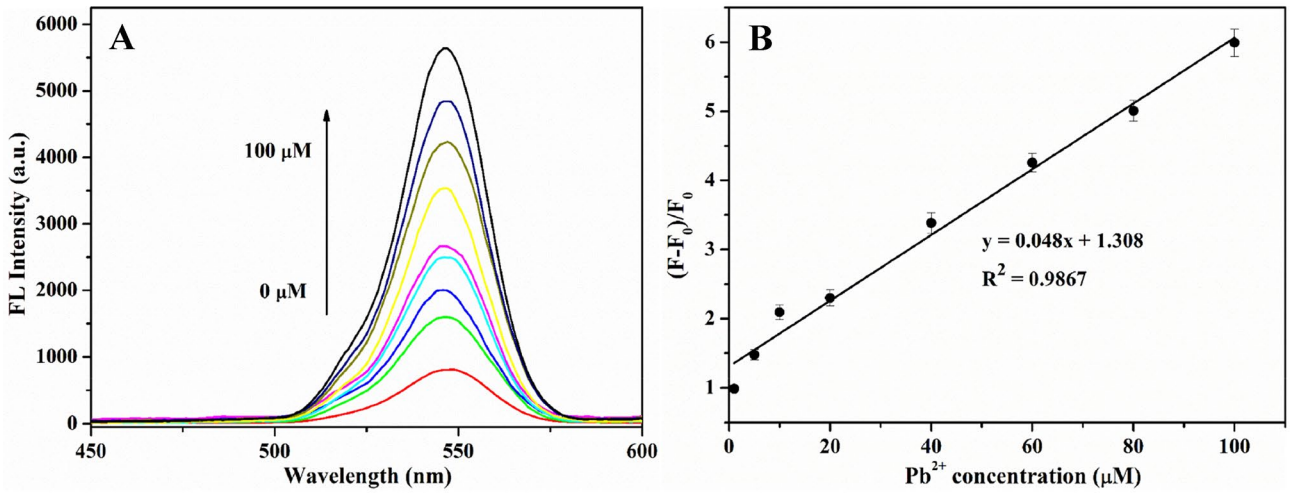


**Fig.3** Fluorescence spectra of upconversion with addition of different concentrations $Pb^{2+}$ (**A**) and the standard curve (**B**). Error bar = SD (n = 3)

**Table 1** Comparison of the analytical performances of different methods for $Pb^{2+}$ detection

| Method | Linear range (μM) | LOD (μM) | Reference |
|---|---|---|---|
| Flame atomic absorption spectrometry | 3–150 | 0.75 | [29] |
| Electrochemical analysis | 0.5–10 | 0.3 | [30] |
| Electrochemical aptasensor | 0.001–0.04 | $0.37 \times 10^{-3}$ | [33] |
| Ccolorimetry | 0.5–25 | 0.5 | [31] |
| Fluorescent sensor | – | 2.23 | [32] |
| Upconversion fluorescence method in this study | 1–100 | 0.5 | – |

a LOD of 0.5 μM attained by the sensor. The characteristics comparison between the fabricated sensor and other reported $Pb^{2+}$ detection methods are captured in Table 1 [29–33]. It is observed from the results that the designed sensor has high detection sensitivity.

## Selectivity analysis

Analysis of the selectivity and specificity of the fabricated nano fluorescent sensor to detect $Pb^{2+}$ was evaluated using common metal ions such as ($Ba^{2+}$, $Cd^{2+}$, $Ca^{2+}$, $Na^{+}$, $Al^{3+}$, $Mg^{2+}$, $K^{+}$, $Zn^{2+}$, $Cu^{2+}$, $Mn^{2+}$, $Fe^{3+}$, $Ag^{+}$, $Fe^{2+}$) as targets. Results shown in Fig. S2, reveal that when all metal ions were added at the same concentration (20 μM) and condition, only $Pb^{2+}$ significantly increased the fluorescence intensity of the detection system at 547 nm, while the fluorescence changes caused by other pesticides were almost insignificant. This indicates that only $Pb^{2+}$ can form a complex with Cys, which results in its dissociation from the assembly and the consequent recovery of upconversion fluorescence. The results suggest that the upconversion fluorescent nanoprobes have good selectivity and specificity for $Pb^{2+}$ detection.

**Table 2** Determination of $Pb^{2+}$ in various spiked samples using the developed method

| Matcha | Addition (μg/g) | Found (μg/g) | Recovery (%) | RSD (%) |
|---|---|---|---|---|
| Sample 1 | 0 | / | / | / |
| Sample 2 | 5 | 4.699 | 93.99 | 5.631 |
| Sample 3 | 15 | 14.275 | 95.16 | 7.717 |
| Sample 4 | 30 | 30.647 | 102.16 | 2.407 |

## Determination of $Pb^{2+}$ in real matcha samples

The practicability of the upconversion fluorescent nanoprobe to detect $Pb^{2+}$ in real samples and its recovery rate in Maccha samples were carried out and the analyzed results captured in Table 2. The detection value of $Pb^{2+}$ obtained was consistent with the standard addition amount and a detection recovery range between 93.99—102.16% with the relative standard deviation of 2.4—7.8% was computed. Additionally, the developed sensor was validated by the traditional inductively coupled plasma mass spectrometry (ICP-MS) based on the same pretreatment process. Table 3 shows that the difference between obtained results of the fabricated

**Table 3** Comparison of the results from ICP-MS and the developed method for $Pb^{2+}$ detection

| Matcha | Found ± SD (μg/g) | | Significance analysis results |
|---|---|---|---|
| | ICP-MS | Present method | |
| Sample 1 | 4.52 ± 0.17 | 3.59 ± 0.16 | No significance ($P = 0.06 > 0.05$) |
| Sample 2 | 6.63 ± 0.24 | 6.28 ± 0.29 | |
| Sample 3 | 3.56 ± 0.23 | 2.68 ± 0.08 | |

Error bar = SD (n = 3)

UCNPs-based sensor and ICP-MS method were not significantly different ($p > 0.05$). The results obtained prove that the fabricated sensor is stable, sensitive and accurate for $Pb^{2+}$ detection and quantification in practical Matcha samples.

## Conclusions

This paper reported on the development of A UCNPs-Cys-AuNRs based FRET biosensor for the determination of $Pb^{2+}$ residues in Matcha samples. The Cys was used as a bridge to connect UCNPs and AuNRs via chemical bond. The resultant fabricated sensor based on this study was deployed to quantitatively detect $Pb^{2+}$ in Matcha samples. When the fabricated sensor was deployed under the optimal conditions, a LOD of 0.5 μM was achieved and a good linear correlation between the relative fluorescence intensity and the concentration of $Pb^{2+}$ within a range of 1–100 μM established. Additionally, it was proven that the resultant sensor yielded a high selectivity and specificity for the detection of $Pb^{2+}$ based on specificity analysis carried out. Finally, the recovery test of $Pb^{2+}$ in actual Matcha samples and the comparison of detection results realized through the use of the fabricated sensor with that of inductively coupled plasma mass spectrometry, revealed the fabricated sensor as simple, fast, accurate and reliable to be deployed for the quality and safety monitoring of $Pb^{2+}$ in Matcha and other food materials.

**Supplementary Information** The online version contains supplementary material available at https://doi.org/10.1007/s11694-021-01054-x.

**Acknowledgements** This work has been financially supported by Jiangsu Agricultural Science and Technology Innovation Fund Grant No. (CX(20)2005), and the Jiangsu Provincial Key Research and Development Program Grant No. (BE2020379).

## Declarations

**Conflict of interest** The authors declare no known competing financial interests or personal relationships that could have appeared to influence the work reported in this paper.

## References

1. H. Karimi-Maleh, M.L. Yola, N. Atar, Y. Orooji, F. Karimi, P. Senthil Kumar, J. Rouhi, M. Baghayeri, A novel detection method for organophosphorus insecticide fenamiphos: molecularly imprinted electrochemical sensor based on core-shell Co3O4@MOF-74 nanocomposite. J Colloid Interface Sci **592**, 174–185 (2021). https://doi.org/10.1016/j.jcis.2021.02.066
2. Z. Shamsadin-Azad, M.A. Taher, S. Cheraghi, H. Karimi-Maleh, A nanostructure voltammetric platform amplified with ionic liquid for determination of tert-butylhydroxyanisole in the presence kojic acid. J Food Meas Charact **13**(3), 1781–1787 (2019). https://doi.org/10.1007/s11694-019-00096-6
3. A. Baghizadeh, H. Karimi-Maleh, Z. Khoshnama, A. Hassankhani, M. Abbasghorbani, A voltammetric sensor for simultaneous determination of vitamin C and vitamin B6 in food samples using ZrO2 nanoparticle/ionic liquids carbon paste electrode. Food Anal Methods **8**(3), 549–557 (2015). https://doi.org/10.1007/s12161-014-9926-3
4. T. Jamali, H. Karimi-Maleh, M.A. Khalilzadeh, A novel nanosensor based on Pt: Co nanoalloy ionic liquid carbon paste electrode for voltammetric determination of vitamin B9 in food samples. LWT Food Sci Technol **57**(2), 679–685 (2014). https://doi.org/10.1016/j.lwt.2014.01.023
5. J. Wang, M. Zareef, P. He, H. Sun, Q. Chen, H. Li, Q. Ouyang, Z. Guo, Z. Zhang, D. Xu, Evaluation of matcha tea quality index using portable NIR spectroscopy coupled with chemometric algorithms. J Sci Food Agri **99**(11), 5019–5027 (2019). https://doi.org/10.1002/jsfa.9743
6. H. Karimi-Maleh, S. Ranjbari, B. Tanhaei, A. Ayati, Y. Orooji, M. Alizadeh, F. Karimi, S. Salmanpour, J. Rouhi, M. Sillanpää, F. Sen, Novel 1-butyl-3-methylimidazolium bromide impregnated chitosan hydrogel beads nanostructure as an efficient nanobio-adsorbent for cationic dye removal: Kinetic study. Environ Res **195**, 110809 (2021). https://doi.org/10.1016/j.envres.2021.110809
7. H. Karimi-Maleh, A. Ayati, S. Ghanbari, Y. Orooji, B. Tanhaei, F. Karimi, M. Alizadeh, J. Rouhi, L. Fu, M. Sillanpää, Recent advances in removal techniques of Cr(VI) toxic ion from aqueous solution: a comprehensive review. J Mol Liq **329**, 115062 (2021). https://doi.org/10.1016/j.molliq.2020.115062
8. H. Karimi-Maleh, A. Ayati, R. Davoodi, B. Tanhaei, F. Karimi, S. Malekmohammadi, Y. Orooji, L. Fu, M. Sillanpää, Recent advances in using of chitosan-based adsorbents for removal of pharmaceutical contaminants: a review. J Clean Prod **291**, 125880 (2021). https://doi.org/10.1016/j.jclepro.2021.125880
9. Q. Ouyang, L. Wang, B. Park, R. Kang, Z. Wang, Q. Chen, Z. Guo, Assessment of matcha sensory quality using hyperspectral microscope imaging technology. LWT-Food Sci Technol **125**, 109254 (2020). https://doi.org/10.1016/j.lwt.2020.109254
10. Z. Lotfi, H.Z. Mousavi, S.M. Sajjadi, Covalently bonded dithiocarbamate-terminated hyperbranched polyamidoamine polymer on magnetic graphene oxide nanosheets as an efficient sorbent for preconcentration and separation of trace levels of some heavy metal ions in food samples. J Food Meas Charact **14**(1), 293–302 (2020). https://doi.org/10.1007/s11694-019-00291-5
11. National Standard of PR China GB/T 34778-2017 Matcha
12. D. Bain, S. Maity, B. Paramanik, A. Patra, Core-size dependent fluorescent gold nanoclusters and ultrasensitive detection of $Pb^{2+}$ ion. ACS Sus Tan Chem Eng **6**, 2334–2343 (2018). https://doi.org/10.1021/acssuschemeng.7b03794
13. Y. Noh, E.-J. Jo, H. Mun, Y.-D. Ahn, M.-G. Kim, Homogeneous and selective detection of cadmium ions by forming fluorescent cadmium-protein nanoclusters. Chemosphere **174**, 524–530 (2017). https://doi.org/10.1016/j.chemosphere.2017.02.025

14. T. Rasheed, M. Bilal, F. Nabeel, H.M.N. Iqbal, C.L. Li, Y.F. Zhou, Fluorescent sensor based models for the detection of environmentally-related toxic heavy metals. Sci Total Environ **615**, 476–485 (2018). https://doi.org/10.1016/j.scitotenv.2017.09.126
15. E. Priyadarshini, N. Pradhan, Gold nanoparticles as efficient sensors in colorimetric detection of toxic metal ions: a review. Sens Actuator B-Chem **238**, 888–902 (2017). https://doi.org/10.1016/j.snb.2016.06.081
16. Y. Yao, H. Wu, J.F. Ping, Simultaneous determination of Cd(II) and Pb(II) ions in honey and milk samples using a single-walled carbon nanohorns modified screen-printed electrochemical sensor. Food Chem **274**, 8–15 (2019). https://doi.org/10.1016/j.foodchem.2018.08.110
17. P.C. Yang, P.H. Lin, C.C. Huang, T. Wu, Y.W. Lin, Determination of Hg(II) based on the inhibited catalytic growth of surface-enhanced Raman scattering-active gold nanoparticles on a patterned hydrophobic paper substrate. Microchem J **157**, 9 (2020). https://doi.org/10.1016/j.microc.2020.104983
18. Y. Liu, Q. Ouyang, H. Li, M. Chen, Z. Zhang, Q. Chen, Turn-on fluoresence sensor for Hg(2+) in food based on FRET between aptamers-functionalized upconversion nanoparticles and gold nanoparticles. J Agric Food Chem **66**(24), 6188–6195 (2018). https://doi.org/10.1021/acs.jafc.8b00546
19. T. Li, S.J. Dong, E.K. Wang, A lead(II)-driven DNA molecular device for turn-on fluorescence detection of lead(II) ion with high selectivity and sensitivity. J Am Chem Soc **132**(38), 13156–13157 (2010). https://doi.org/10.1021/ja105849m
20. H. Liu, H. Wang, L. Zhang, Y.J. Sang, F. Pu, J.S. Ren, X.G. Qu, Fe(III)-oxidized graphitic carbon nitride nanosheets as a sensitive fluorescent sensor for detection and imaging of fluoride ions. Sens Actuator B-Chem **321**, 7 (2020). https://doi.org/10.1016/j.snb.2020.128630
21. P. Wang, H. Li, M.M. Hassan, Z. Guo, Z.Z. Zhang, Q. Chen, Fabricating an acetylcholinesterase modulated UCNPs-Cu(2+) fluorescence biosensor for ultrasensitive detection of organophosphorus pesticides-diazinon in food. J Agric Food Chem **67**(14), 4071–4079 (2019). https://doi.org/10.1021/acs.jafc.8b07201
22. Y. Gong, Y. Zheng, B. Jin, M. You, J. Wang, X. Li, M. Lin, F. Xu, F. Li, A portable and universal upconversion nanoparticle-based lateral flow assay platform for point-of-care testing. Talanta **201**, 126–133 (2019). https://doi.org/10.1016/j.talanta.2019.03.105
23. L. Shi, J. Hu, X. Wu, S. Zhan, S. Hu, Z. Tang, M. Chen, Y. Liu, Upconversion core/shell nanoparticles with lowered surface quenching for fluorescence detection of Hg(2+) ions. Dalton Trans **47**(46), 16445–16452 (2018). https://doi.org/10.1039/c8dt02853b
24. A.N. Vijayan, Z. Liu, H. Zhao, P. Zhang, Nicking enzyme-assisted signal-amplifiable Hg(2+) detection using upconversion nanoparticles. Anal Chim Acta **1072**, 75–80 (2019). https://doi.org/10.1016/j.aca.2019.05.001
25. Y. Wang, M. Lv, Z. Chen, Z. Deng, N. Liu, J. Fan, W. Zhang, A fluorescence resonance energy transfer probe based on DNA-modified upconversion and gold nanoparticles for detection of lead ions. Front Chem **8**, 238 (2020). https://doi.org/10.3389/fchem.2020.00238
26. W. Pan, J. Zhao, Q. Chen, Fabricating upconversion fluorescent probes for rapidly sensing foodborne pathogens. J Agric Food Chem **63**(36), 8068–8074 (2015). https://doi.org/10.1021/acs.jafc.5b02331
27. N. Bogdan, F. Vetrone, G.A. Ozin, J.A. Capobianco, Synthesis of ligand-free colloidally stable water dispersible brightly luminescent lanthanide-doped upconverting nanoparticles. Nano Lett **11**(2), 835–840 (2011). https://doi.org/10.1021/nl1041929
28. X.C. Ye, Y.Z. Gao, J. Chen, D.C. Reifsnyder, C. Zheng, C.B. Murray, Seeded growth of monodisperse gold nanorods using bromide-free surfactant mixtures. Nano Lett **13**(5), 2163–2171 (2013). https://doi.org/10.1021/nl400653s
29. H. Ebrahimzadeh, M. Behbahani, A novel lead imprinted polymer as the selective solid phase for extraction and trace detection of lead ions by flame atomic absorption spectrophotometry: synthesis, characterization and analytical application. Arab J Chem **77**, 2499–2508 (2013). https://doi.org/10.1016/j.arabjc.2013.09.017
30. Y. Xiao, A.A. Rowe, K.W. Plaxco, Electrochemical detection of parts-per-billion lead via an electrode-bound DNAzyme assembly. J Am Chem Soc **129**(2), 262–263 (2007). https://doi.org/10.1021/ja067278x
31. N.A. Khan, A. Niaz, M.I. Zaman, F.A. Khan, M. Nisar-Ul-Haq, M. Tariq, Sensitive and selective colorimetric detection of Pb 2+ by silver nanoparticles synthesized from Aconitum violaceum plant leaf extract. Mater Res Bull **102**, 330–336 (2018). https://doi.org/10.1016/j.materresbull.2018.02.050
32. M. Rahimi, A. Amini, H. Behmadi, Novel symmetric Schiff-base benzobisthiazole-salicylidene derivative with fluorescence turn-on behavior for detecting Pb2+ ion. J Photochem Photobiol A-Chem **388**, 11 (2020). https://doi.org/10.1016/j.jphotochem.2019.112190
33. M. Adabi, Detection of lead ions using an electrochemical aptasensor. Nanomed Res J **4**(4), 247–252 (2019). https://doi.org/10.22034/nmrj.2019.04.007